

Multi-Source Thermal Model Describing Transverse Momentum Spectra of Final-State Particles in High Energy Collisions

Fu-Hu Liu*, Jia-Yu Chen, Qiang Zhang

*Institute of Theoretical Physics, State Key Laboratory of Quantum Optics and Quantum Optics Devices
& Collaborative Innovation Center of Extreme Optics, Shanxi University, Taiyuan 030006, China*

Abstract: In this mini review article, the transverse momentum spectra of final-state particles produced in high energy hadron-hadron, hadron-nucleus, and nucleus-nucleus collisions described by the multi-source thermal model at the quark or parton level is summarized. In the model, the participant or contributor quarks or partons are considered to contribute together to the transverse momentum distribution of final-state particles with different modes of contributions. The concrete mode of contribution is generally determined by the difference of azimuthal angles of contributor partons in their emissions.

Keywords: Transverse momentum spectra, multi-source thermal model, Monte Carlo method, convolution method, revised Tsallis-like function

PACS numbers: 12.40.Ee, 13.85.Hd, 24.10.Pa

I. INTRODUCTION

In high energy hadron-hadron, hadron-nucleus, and nucleus-nucleus collisions, abundant data measured in experiments reflect colorful mechanisms of particle production and system evolution [1–3]. As an important issue, the transverse momentum spectra contain the information of the excitation degree of emission source, and show the similarity, commonality, and universality in particle productions [4–11]. The multi-source thermal model [12–16] proposed by us is successful in describing the distributions of some quantities such as multiplicities, isotopic cross-sections, (pseudo)rapidities, transverse energies, azimuthal angles, transverse momenta, etc. In the model, the nucleons or nucleon clusters were regarded as the multi-source and the Boltzmann-Gibbs statistics was used in describing a given source.

The multi-source thermal model was proposed according to the single-, two-, and three-fireball models [17–24], as well as the multi-source ideal-gas model or the cylinder model [25–28]. Recently, the Boltzmann-Gibbs statistics used in the model was replaced by the Tsallis statistics, and the multi-source of fireballs (nucleons or nucleon clusters) was replaced by the multi-source of participant or contributor quarks or partons [29–31]. Here,

the single component distribution from the Boltzmann-Gibbs statistics is not enough to fit the transverse momentum spectra. Two- or three-component distribution is needed, which results in the temperature fluctuations and is covered by the Tsallis distribution with less parameters [32].

It should be noted that in the multi-source thermal model the sources changed from fireballs to participant partons means that the smaller contributor units at the deeper level are used. This is an important progress or improvement in the viewpoint of the model. A fireball may contain lots of partons, and the partons are the underlying units of collisions. The latest version of the model was tested firstly by the transverse momentum spectra of final-state particles [29–31]. Some quantities such as the temperature of parton source and the average transverse flow velocity of partons can be extracted from describing the transverse momentum spectra. In view of the latest progress of the model, it is necessary to review and summarize it in some way.

The multi-source thermal model is a static thermodynamical and statistical model. Although the dynamical evolution process of the interacting system cannot be described by the model, some useful quantities can be extracted from the comparisons of the model with experimental data. The dependences of the concerned quantities on collision energy, event centrality, system size, particle rapidity, particle mass, and quark mass can

*E-mail: fuhuliu@163.com; fuhuliu@sxu.edu.cn

be obtained. The sudden changes of these dependences are expected to relate to the formation of quark-gluon plasma (QGP) or quark matter [31, 33–38]. It is believed that QGP was produced in a hot and dense environment formed in the experiments at the relativistic heavy ion collider (RHIC) [39–44] and the large hadron collider (LHC) [45–48]. As the strongly interacting partonic medium formed at the RHIC and LHC, QGP was predicted by the quantum chromodynamics (QCD) theory which describes the strong interactions [49–53].

This mini review article will summarize the method for describing the transverse momentum spectra of final-state particles produced in high energy collisions in the framework of multi-source thermal model at the parton level. The contributions of the contributor partons are considered in different ways where different azimuthal differences are used. The azimuthal difference may be various values in $[0, 2\pi]$ in general, or in particular 0 or π if the contributions of two partons are parallel, or $\pi/2$ if the contributions of two partons are perpendicular. Although the azimuthal difference may be particular value, the azimuthal angles are independent and there is no sorting for them.

The rest of this article is structured as follows. The physics picture and formalism expression of the multi-source thermal model at the parton level are described in Section 2. Implementation and discussion are given in Section 3. In Section 4, the summary and conclusion of this article are given.

II. PICTURE AND FORMALISM

In high energy hadron-hadron, hadron-nucleus, and nucleus-nucleus collisions, many final-state particles are produced in collision process and measured in experiments. Meanwhile, a few fragments which are nucleons or nucleon clusters from the spectator fragmentation are produced in the final state in hadron-nucleus and nucleus-nucleus collisions. In collisions at very high energies, a few jets are produced, which consists of many particles. In most cases, final-state particles are main products in high energy collisions.

To describe the production of final-state particles, it is natural that a single-fireball is assumed to form in the collisions of projectile and target hadrons (or nuclei) at a few GeV which is not too high energy. In the rest frame of the fireball, one may assume that the particles are emitted isotropically, as discussed in the multi-source thermal model [12–16]. However, the particles are anisotropic in experiments. Then, the single-fireball is needed to extend to a two-fireball [17, 18] in which one is from the

projectile hadron (or nucleus) and the other one is from the target hadron (or nucleus), or a three-fireball [19–24] which consists of the projectile, central, and target fireballs. Although the particles are isotropic in the rest frame of each fireball, the experimental spectra can be anisotropic due to the motion of the fireball.

Further, the three-fireball is extended to a thermalized cylinder or fire-cylinder [54–57] which is formed due to the penetrations of projectile and target hadrons (or nuclei) in the collisions at higher energy (dozens of GeV and TeV). The single-cylinder can be extended to a two-cylinder [26, 27] in which one is from the projectile hadron (or nucleus) and the other one is from the target hadron (or nucleus). The two cylinders may overlap or separate each other. In the rapidity space, the emission points with the same rapidity in the cylinder(s) consist of a large emission source. In the rest frame of the considered large emission source, the particles are assumed to emit isotropically.

Generally, a given particle is produced from the interactions of two or three contributor partons. Concretely, a meson (baryon) is produced from the interactions of two (three) constituent or contributor quarks, while a lepton is produced from the interactions of two contributor quarks or gluons. Here, the additive quark model [58–62] is considered for part case, in which the meson (baryon) consists of two (three) constituent quarks within the model, but these are not numbers of quarks producing meson (baryon) via their (quarks) interactions which are additionally considered in the multi-source thermal model [12–16]. In most cases, more partons may take part in the interactions. However, only two or three partons take part in the main role in the production of a given particle. Of course, for a tetraquark or pentaquark state, one naturally considers four or five constituent quarks. As an approximate treatment, two contributor heavy quarks may also produce a multi-quark state or an arbitrary jet.

Let p_T and p_{t1} (p_{t2}) denote the transverse momentum of given particle and the contribution amount of the first (second) parton to p_T respectively. The probability density function obeyed by p_T and p_{t1} (p_{t2}) are $f(p_T)$ and $f_1(p_{t1})$ ($f_2(p_{t2})$) respectively, where the variables such as the temperature parameter T and entropy index q in the Tsallis statistics are not listed in the functions for convenience. One may study the relation between p_T and p_{t1} (p_{t2}), as well as $f(p_T)$ and $f_1(p_{t1})$ ($f_2(p_{t2})$) according to the difference between the azimuthal angle ϕ_1 of the first parton and the azimuthal angle ϕ_2 of the second parton in the emission.

We would like to explain the azimuthal angle in the right-handed Cartesian coordinate system $O-xyz$ in de-

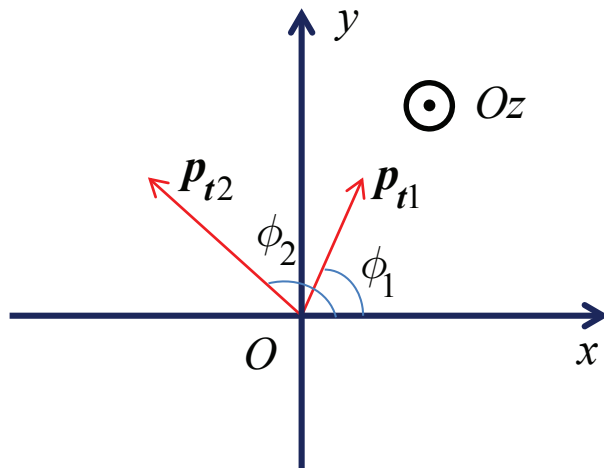


Fig. 1. The right-handed Cartesian coordinate system $Oxyz$. The beam direction which is along the Oz axis points from the inside to the outside. The reaction plane is the plane xOz , and the transverse plane is the plane xOy which is perpendicular to the beam direction. In the figure, ϕ_1 (ϕ_2) is the angle of vector \mathbf{p}_{t1} (\mathbf{p}_{t2}) measured with respect to the Ox axis in the plane xOy .

tail. For clarity, Figure 1 shows the scheme of kinematic variables in the transverse plane xOy , where the beam direction which is along the Oz axis points from the inside to the outside and the reaction plane is xOz . Here, ϕ_1 (ϕ_2) is the angle of vector \mathbf{p}_{t1} (\mathbf{p}_{t2}) measured with respect to the Ox axis in the transverse plane xOy which is perpendicular to the beam direction Oz axis.

In the following text, a general case and two particular cases are discussed in subsections i)–iii) successively. Then, the connection of p_T to the rapidity y and pseudorapidity η is discussed in subsection iv). For each issue, the basic method and formalism are presented.

i) General case: various azimuths

For any difference between ϕ_1 and ϕ_2 , the analytic relation between $f(p_T)$ and $f_1(p_{t1})$ ($f_2(p_{t2})$) is hard to obtain. Instead, one may use the Monte carlo method to perform the calculations. Based on $f_1(p_{t1})$ and $f_2(p_{t2})$, one may obtain p_{t1} and p_{t2} firstly. In fact, in the Monte Carlo method, let $r_{1,2,3,4}$ denote random numbers distributed evenly in $[0, 1]$. One may extract p_{t1} and p_{t2} according to

$$\int_0^{p_{t1}} f_1(p'_{t1}) dp'_{t1} < r_1 \leq \int_0^{p_{t1} + \delta p_{t1}} f_1(p'_{t1}) dp'_{t1}, \quad (1)$$

$$\int_0^{p_{t2}} f_2(p'_{t2}) dp'_{t2} < r_2 \leq \int_0^{p_{t2} + \delta p_{t2}} f_2(p'_{t2}) dp'_{t2}. \quad (2)$$

Meanwhile, one may obtain ϕ_1 and ϕ_2 due to the assumption of isotropy in the source rest frame. That is

$$\phi_1 = 2\pi r_3, \quad (3)$$

$$\phi_2 = 2\pi r_4 \quad (4)$$

in the Monte Carlo method, where ϕ_1 (ϕ_2) distributes evenly in $[0, 2\pi]$.

Because isotropic azimuth obeys the uniform distribution, $f_\phi(\phi) = 1/(2\pi)$, in $[0, 2\pi]$ in the transverse plane, the expressions of Eqs. (3) and (4) are natural. It should be noted that both ϕ_1 and ϕ_2 are the independent random numbers distributed evenly in $[0, 2\pi]$ due to the fact that they come from the independent random numbers r_3 and r_4 distributed evenly in $[0, 1]$ respectively. There is no sorting for ϕ_1 and ϕ_2 when they are performed through Eqs. (3) and (4) respectively. Different lower footmarks are used for the two azimuths due to different values. In fact, Eqs. (3) and (4) indeed describe isotropic azimuth respectively, if $\int_0^{\phi_1} f_\phi(\phi') d\phi' = r_3$ and $\int_0^{\phi_2} f_\phi(\phi') d\phi' = r_4$ are solved. In the Monte Carlo calculations in the multi-source thermal model [12–16], ϕ , but not $\cos \phi$, is used because both $\cos \phi$ and $\sin \phi$ can be used more easily.

The two components p_x and p_y , as well as p_T itself can be given by

$$p_x = p_{t1} \cos \phi_1 + p_{t2} \cos \phi_2, \quad (5)$$

$$p_y = p_{t1} \sin \phi_1 + p_{t2} \sin \phi_2, \quad (6)$$

$$p_T = \sqrt{p_x^2 + p_y^2} \\ = \sqrt{p_{t1}^2 + p_{t2}^2 + 2p_{t1}p_{t2} \cos |\phi_1 - \phi_2|}. \quad (7)$$

Then, the probability density function, $(1/N)dN/dp_T$, of p_T can be obtained by the statistics, where N denotes the number of particles. For the frequently-used experimental spectrum, $(1/2\pi p_T)d^2N/dp_T dy$, and other forms, the

statistical method is also available to obtain the forms correspondingly.

The above method can be easily extended to the case of three contributor partons. The quantities p_{t3} , $f_3(p_{t3})$, and ϕ_3 related to the third component can be obtained by the same method. For the case of more partons, the method is also applicable. What one does is considering the third or more components in the expression of p_x and p_y . In fact, including the third parton, one has more equations

$$\int_0^{p_{t3}} f_3(p'_{t3}) dp'_{t3} < r_5 \leq \int_0^{p_{t3} + \delta p_{t3}} f_3(p'_{t3}) dp'_{t3}, \quad (8)$$

$$\phi_3 = 2\pi r_6, \quad (9)$$

where $r_{5,6}$ are random numbers distributed evenly in $[0, 1]$ due to the requirement in the Monte Carlo method. The two components p_x and p_y are improved by

$$p_x = p_{t1} \cos \phi_1 + p_{t2} \cos \phi_2 + p_{t3} \cos \phi_3, \quad (10)$$

$$p_y = p_{t1} \sin \phi_1 + p_{t2} \sin \phi_2 + p_{t3} \sin \phi_3, \quad (11)$$

in which one more item is added. One has

$$\begin{aligned} p_T &= \sqrt{p_x^2 + p_y^2} \\ &= (p_{t1}^2 + p_{t2}^2 + p_{t3}^2 + 2p_{t1}p_{t2} \cos |\phi_1 - \phi_2| \\ &\quad + 2p_{t1}p_{t3} \cos |\phi_1 - \phi_3| + 2p_{t2}p_{t3} \cos |\phi_2 - \phi_3|)^{1/2}. \end{aligned} \quad (12)$$

The case of more partons can be conveniently considered by the frequently-used method of vector synthesis.

ii) Particular case: parallel transverse momenta

For a particular case of $\phi_1 - \phi_2 = 0$, one has $p_T = p_{t1} + p_{t2}$. The Monte Carlo method discussed above is naturally applicable. In addition, the analytic relation between $f(p_T)$ and $f_1(p_{t1})$ ($f_2(p_{t2})$) is easy to obtain [29, 30]. In fact, $f(p_T)$ is the convolution of $f_1(p_{t1})$ and $f_2(p_{t2})$. One has

$$\begin{aligned} f(p_T) &= \int_0^{p_T} f_1(p_{t1}) f_2(p_T - p_{t1}) dp_{t1} \\ &= \int_0^{p_T} f_2(p_{t2}) f_1(p_T - p_{t2}) dp_{t2}. \end{aligned} \quad (13)$$

If the case of three contributor partons with the same azimuthal angle is considered, one has $p_T = p_{t1} + p_{t2} + p_{t3}$. Except the Monte Carlo method, the convolution method is also useable. One has the convolution of $f_1(p_{t1})$ and $f_2(p_{t2})$ to be

$$\begin{aligned} f_{12}(p_{t12}) &= \int_0^{p_{t12}} f_1(p_{t1}) f_2(p_{t12} - p_{t1}) dp_{t1} \\ &= \int_0^{p_{t12}} f_2(p_{t2}) f_1(p_{t12} - p_{t2}) dp_{t2}. \end{aligned} \quad (14)$$

The convolution of $f_{12}(p_{t12})$ and the third function $f_3(p_{t3})$ is

$$\begin{aligned} f(p_T) &= \int_0^{p_T} f_{12}(p_{t12}) f_3(p_T - p_{t12}) dp_{t12} \\ &= \int_0^{p_T} f_3(p_{t3}) f_{12}(p_T - p_{t3}) dp_{t3}. \end{aligned} \quad (15)$$

The case of more partons can be considered by the convolution method step by step [29, 30].

iii) Particular case: vertical transverse momenta

For a particular case of $|\phi_1 - \phi_2| = \pi/2$, one has $p_T = \sqrt{p_{t1}^2 + p_{t2}^2}$. The Monte Carlo method discussed above is naturally applicable. In addition, the analytic relation between $f(p_T)$ and $f_1(p_{t1})$ ($f_2(p_{t2})$) is easy to obtain [31, 63, 64]. Let ϕ (or $\pi/2 - \phi$) denote the azimuthal angle of the vector \mathbf{p}_T relative to the vector \mathbf{p}_{t1} (or the vector \mathbf{p}_{t2}). One has the united probability density function of p_T and ϕ to be

$$\begin{aligned} f_{p_T, \phi}(p_T, \phi) &= p_T f_{1,2}(p_{t1}, p_{t2}) \\ &= p_T f_1(p_{t1}) f_2(p_{t2}) \\ &= p_T f_1(p_T \cos \phi) f_2(p_T \sin \phi), \end{aligned} \quad (16)$$

where $f_{1,2}(p_{t1}, p_{t2})$ is the united probability density function of p_{t1} and p_{t2} . By integrating ϕ , one has

$$\begin{aligned} f(p_T) &= \int_0^{2\pi} f_{p_T, \phi}(p_T, \phi) d\phi \\ &= p_T \int_0^{2\pi} f_1(p_T \cos \phi) f_2(p_T \sin \phi) d\phi. \end{aligned} \quad (17)$$

For the case of three partons, if the synthesis of \mathbf{p}_{t1} and \mathbf{p}_{t2} is coincidentally perpendicular to the vector \mathbf{p}_{t3} , the method of united probability density function is still applicable. Let the vector \mathbf{p}_{t12} denote the synthesis of \mathbf{p}_{t1} and \mathbf{p}_{t2} , ϕ_{12} denote the azimuthal angle of \mathbf{p}_{t12} relative to \mathbf{p}_{t1} , and ϕ' denote the azimuthal angle of \mathbf{p}_T relative to \mathbf{p}_{t12} . The united probability density function of p_{t12} and ϕ_{12} is

$$\begin{aligned} f_{p_{t12}, \phi_{12}}(p_{t12}, \phi_{12}) &= p_{t12} f_{1,2}(p_{t1}, p_{t2}) \\ &= p_{t12} f_1(p_{t1}) f_2(p_{t2}) \\ &= p_{t12} f_1(p_T \cos \phi_{12}) f_2(p_T \sin \phi_{12}). \end{aligned} \quad (18)$$

By integrating ϕ_{12} , one has

$$\begin{aligned} f_{12}(p_{t12}) &= \int_0^{2\pi} f_{p_{t12}, \phi_{12}}(p_{t12}, \phi_{12}) d\phi_{12} \\ &= p_{t12} \int_0^{2\pi} f_1(p_{t12} \cos \phi_{12}) f_2(p_{t12} \sin \phi_{12}) d\phi_{12}. \end{aligned} \quad (19)$$

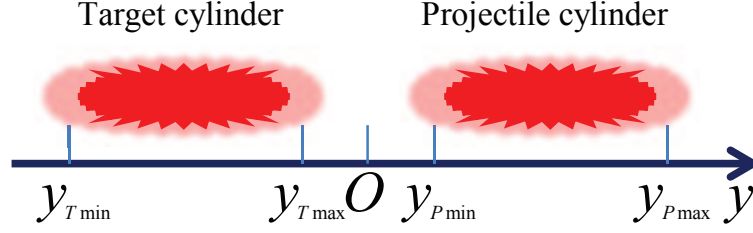


Fig. 2. The relative positions of $y_{P \min}$, $y_{P \max}$, $y_{T \min}$, and $y_{T \max}$ in the rapidity space. The projectile cylinder is assumed to appear on the right side, while the target cylinder appears on the left side.

The united probability density function of p_T and ϕ' is

$$\begin{aligned} f_{p_T, \phi'}(p_T, \phi') &= p_T f_{12,3}(p_{t12}, p_{t3}) \\ &= p_T f_{12}(p_{t12}) f_3(p_{t3}) \\ &= p_T f_{12}(p_T \cos \phi') f_3(p_T \sin \phi'), \end{aligned} \quad (20)$$

where $f_{12,3}(p_{t12}, p_{t3})$ is the united probability density function of p_{t12} and p_{t3} . By integrating ϕ' , one has

$$\begin{aligned} f(p_T) &= \int_0^{2\pi} f_{p_T, \phi'}(p_T, \phi') d\phi' \\ &= p_T \int_0^{2\pi} f_{12}(p_T \cos \phi') f_3(p_T \sin \phi') d\phi'. \end{aligned} \quad (21)$$

The case of more partons can be considered by the method of united probability density function step by step [31, 63, 64].

iv) Connection of p_T to (pseudo)rapidity

In the rapidity space, the projectile cylinder is assumed to stay in the rapidity range $[y_{P \min}, y_{P \max}]$, and the target cylinder stays in the rapidity range $[y_{T \min}, y_{T \max}]$. Figure 2 gives the relative positions of the four rapidities. It assumes that the projectile (target) comes from the left (right) side and the projectile (target) cylinder appears on the right (left) side. If $y_{P \min} < y_{T \max}$, the two cylinders overlap. If $y_{P \min} > y_{T \max}$, there is a gap between the two cylinders. If $y_{P \min} = y_{T \max}$, the two cylinders are connected into one. For symmetrical collisions, one has the relations: $y_{P \max} - y_{P \min} = y_{T \max} - y_{T \min}$, $y_{P \min} = -y_{T \max}$, $y_{P \max} = -y_{T \min}$. These relations reduce the number of parameters.

In the Monte carlo method, let $R_{1,2}$ denote random numbers distributed evenly in $[0, 1]$. One has the rapidity y_x of the emission source distributed evenly in

$[y_{P \min}, y_{P \max}]$ and $[y_{T \min}, y_{T \max}]$ to be

$$y_x = y_{P \min} + (y_{P \max} - y_{P \min}) R_1, \quad (22)$$

$$y_x = y_{T \min} + (y_{T \max} - y_{T \min}) R_2, \quad (23)$$

respectively.

In the source rest frame, in the case of isotropic emission, the probability density function, $f_{\theta'}(\theta')$, of the emission angle, θ' , of the considered particle obeys the half sine function, $(1/2) \sin \theta'$, which results in

$$\theta' = 2 \arcsin \sqrt{R_3}, \quad (24)$$

where R_3 denotes random number distributed evenly in $[0, 1]$. Then, one has the momentum p' , longitudinal momentum p'_z , and energy E' to be

$$p' = p_T \csc \theta', \quad (25)$$

$$p'_z = p_T \cot \theta', \quad (26)$$

$$E' = \sqrt{p'^2 + m_0^2}, \quad (27)$$

where m_0 is the rest mass of the considered particle.

The rapidity y' in the source rest frame is

$$y' = \frac{1}{2} \ln \left(\frac{E' + p'_z}{E' - p'_z} \right). \quad (28)$$

The rapidity y measured in experiments is

$$y = y' + y_x. \quad (29)$$

The rapidity distribution, $(1/N) dN/dy$, can be obtained by the statistics.

In terms of the pseudorapidity, η , measured in experiments, one needs the longitudinal momentum

$$p_z = \sqrt{p_T^2 + m_0^2} \sinh y. \quad (30)$$

Then, the emission angle

$$\theta = \arctan \frac{p_T}{p_z} \quad (31)$$

and the pseudorapidity

$$\eta = -\ln \tan \frac{\theta}{2}. \quad (32)$$

The pseudorapidity distribution, $(1/N)dN/d\eta$, can be obtained by the statistics. Here, η and y , and their distributions, are obtained respectively.

In particular, if the analytical expression, $f_{y'}(y')$, of the probability density function for y' in the source rest frame is available, one has the analytical expression, $f_y(y)$, of the probability density function for y in experiments to be

$$f_y(y) = \frac{k}{y_{P \max} - y_{P \min}} \int_{y_{P \min}}^{y_{P \max}} f_{y'}(y - y_x) dy_x + \frac{1 - k}{y_{T \max} - y_{T \min}} \int_{y_{T \min}}^{y_{T \max}} f_{y'}(y - y_x) dy_x, \quad (33)$$

where k ($1 - k$) denotes the contribution fraction of the projectile (target) cylinder.

III. IMPLEMENTATION AND DISCUSSION

In the general case and the two particular cases discussed above, one needs firstly to choose $f_1(p_{t1})$, $f_2(p_{t2})$, and $f_3(p_{t3})$ for contributor partons. The three functions should be the same in form with the same or different parameter values. To find a suitable function, one has tried many attempts. Finally, one finds that the Tsallis function is a possible candidate, though it has different forms in the literature, including in high energy physics [65–69]. In particular, the revised Tsallis-like function is a suitable choice according to our recent attempts [29, 30]. Then, one has

$$f_i(p_{ti}) = C_i p_{ti}^{a_0} \left[1 - \frac{1 - q}{T} (m_{ti} - m_{0i}) \right]^{q/(1-q)}, \quad (34)$$

where the subscript i is for the i -th contributor parton, $m_{ti} = \sqrt{p_{ti}^2 + m_{0i}^2}$ is the transverse mass, m_{0i} is the empirical constituent mass, T is the effective temperature, q is the entropy index, a_0 is the revised index, and C_i is the normalization constant. The power index $q/(1 - q)$ is used to cater to the consistency of thermodynamics from the probabilities of microstates and the maximum entropy principle.

In Eq. (34), the entropy index q describes the departure degree of the system from the equilibrium, or the degree of non-equilibrium of the system. Generally, $q = 1$ corresponds to the equilibrium, $1 < q < 1.25$ means an approximate equilibrium. As an insensitive quantity, q is not too large even at very high energy, which means the approximate equilibrium of the system. Empirically, for

both the quarks and gluons, m_{0i} is regarded as the constituent masses of quarks, but not other mass such as the bare or the effective quark mass. For light (heavy) particles, m_{0i} is taken to be the constituent masses of light (heavy) quarks. For various jets, m_{0i} is taken to be the constituent masses of heavy quarks. The specific quarks (with different m_{0i}) depend on the types of particles and jets, which is used in our recent work [29–31, 70].

The above revised Tsallis-like function is possibly to be revised again for different cases. For example, for the particular case of parallel transverse momenta, it is suitable. For the particular case of vertical transverse momenta [31, 63], one has another revision

$$f_i(p_{ti}) = C_i m_{ti}^{a_0} \left[1 - \frac{1 - q}{T} (m_{ti} - m_{0i}) \right]^{q/(1-q)}. \quad (35)$$

The two revisions are empirical expressions. The first revision can be used in the second particular case approximately. Meanwhile, the second revision can be used in the first particular case approximately.

The above concrete expressions of $f_i(p_{ti})$ are for mid-rapidity (mid- $y_i \approx 0$) only. Meanwhile, the chemical potential (μ_i) is not included. To include non-mid- y_i and non-zero μ_i , one may use $m_{ti} \cosh y_i - \mu_i - m_{0i}$ to replace $m_{ti} - m_{0i}$ expediently, and perform an integral for y_i from the minimum to maximum y_i . If the range from the minimum to maximum y_i does not cover the mid- y_i , one may shift the range to cover the mid- y_i simply. This performance is to exclude the contribution of directed and longitudinal motion of the emission source from the temperature parameter.

The parameter T is called the effective temperature, but not the (physical) temperature, due to the fact that the contribution of flow effect is not excluded. To dissociate the contributions of thermal motion and flow effect related to i -th contributor parton, one may use an alternative method in which the intercept in the linear relation of T versus m_{0i} is regarded as the kinetic freeze-out temperature, and the slope in the linear relation of average p_{ti} ($\langle p_{ti} \rangle$) versus average moving mass (\overline{m}_i) or average energy (\overline{E}_i) in the source rest frame is regarded as the average transverse flow velocity [71–76].

The above alternative method of intercept-slope works well at the particle level. It does not work well at the parton level due to limited type and undefined mass of partons. For example, in many cases, one has only one or two types of partons available in the analysis, and the masses of up and down quarks are almost the same. In addition, the mass of gluon has no strict definition in the analysis, though one may regard it as the constituent mass of light quarks approximately if needed. These limited type and undefined mass of partons result in the

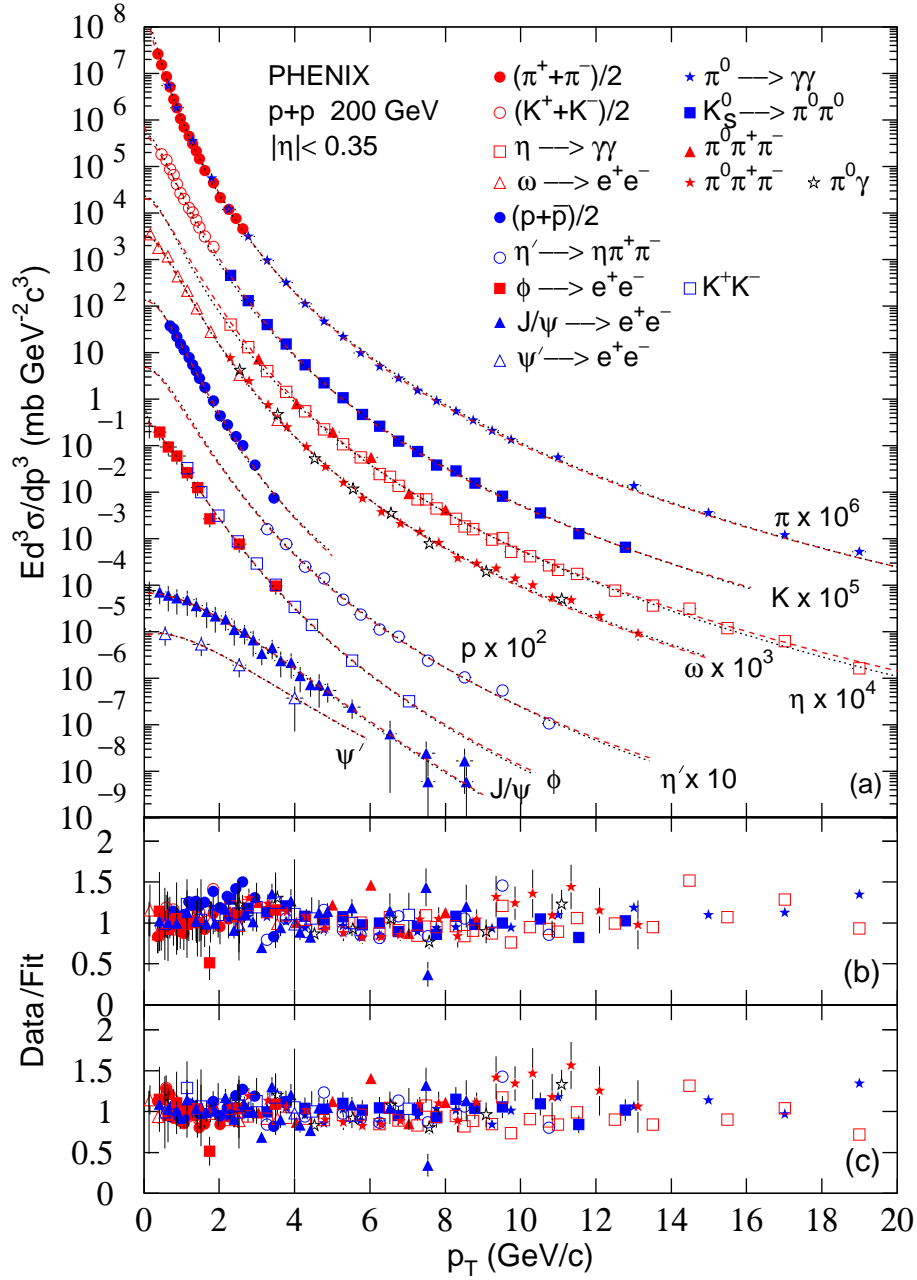


Fig. 3. (a) The invariant cross-sections of various hadrons with given combinations and decay channels produced in p+p collisions at 200 GeV. The symbols represent the experimental data measured by the PHENIX Collaboration [81], and the dotted and dashed curves are the fitted results by using the revised Tsallis distribution [with the power index $1/(1-q)$ in Eq. (34)] and the convolution, respectively [29]. (b) The ratio of data to fit obtained from the dotted curves. (c) The ratio of data to fit obtained from the dashed curves. Detailed information and related parameters can be found in ref. [29] from where the figure is cited.

application of the alternative method of intercept-slope not to be on the right way.

To obtain the kinetic freeze-out temperature T_0 and the average transverse flow velocity $\langle\beta_t\rangle$ at the parton level, one may perform a Lorentz-like transformation for p_{ti} and m_{ti} in the concrete expressions of $f_i(p_{ti})$. For

clarity, p_{ti} , m_{ti} , and $f_i(p_{ti})$ in Eqs. (34) and (35) are substituted by p'_{ti} , m'_{ti} , and $f'_i(p'_{ti})$, respectively. One has the transformations

$$|p'_{ti}| = \langle\gamma_t\rangle|p_{ti} - m_{ti}\langle\beta_t\rangle|, \quad (36)$$

$$m'_{ti} = \langle\gamma_t\rangle(m_{ti} - p_{ti}\langle\beta_t\rangle), \quad (37)$$

where $\langle\gamma_t\rangle = 1/\sqrt{1-\langle\beta_t\rangle^2}$ [77–80] is the Lorentz-like factor. It should be noted that the Lorentz-like, but not the Lorentz, transformation or factor is called due to the fact that $\langle\beta_t\rangle$ is used, but not β_t . The absolute value $|p_{ti} - m_{ti}\langle\beta_t\rangle|$ is used due to p'_{ti} being positive and $p_{ti} - m_{ti}\langle\beta_t\rangle$ being possibly negative in low- p_{ti} region. After the conversion, one has

$$\begin{aligned} f_i(p_{ti}) &= f_{i'}(p'_{ti}) \left| \frac{dp'_{ti}}{dp_{ti}} \right| \\ &= f_{i'}(\langle\gamma_t\rangle|p_{ti} - m_{ti}\langle\beta_t\rangle|) \langle\gamma_t\rangle \frac{m_{ti} - p_{ti}\langle\beta_t\rangle}{m_{ti}} \quad (38) \end{aligned}$$

because of the probability conservation, where $f_{i'}(p'_{ti})$ is given by Eqs. (34) and (35) due to the substitution before the conversion. After the conversion, the parameter T in the concrete expressions of $f_i(p_{ti})$ is the kinetic freeze-out temperature T_0 .

The Monte Carlo method is suitable to the general case where the difference between azimuthal angles are various. However, the calculated results have no value or have large fluctuations in high- p_T region, even the total number of simulated particles is very large. One needs to improve the method of simulated calculation, for example, using the piecewise simulation for the low- and high- p_T regions respectively. By contrary, the analytical method suited to the parallel or perpendicular situation describes the spectra in whole p_T region smoothly.

Our recent studies [29–31, 70] show that the convolution method for the parallel case is more easier to fit the wide p_T spectra. A two-component function is needed for the wide p_T spectra if the method of united probability density function for the perpendicular case is used. The Monte Carlo method for the general case seems more reasonable, though more computing resources are needed. According to the fitting experience, to fit the spectra in wide p_T range, the convolution method for the parallel case is more convenient.

As an example of the application of the multi-source thermal model, the p_T spectra (the invariant cross-section), $Ed^3\sigma/dp^3$, of various hadrons with given combinations and decay channels produced in proton-proton (p+p) collisions at center-of-mass energy of 200 GeV is displayed in Figure 3 which is cited from ref. [29]. In panel (a), the symbols represent the experimental data measured by the PHENIX Collaboration [81], and the dotted and dashed curves are the fitted results by using the revised Tsallis distribution [with the power index $1/(1-q)$ which has a slight difference from Eq. (34)] and the convolution, respectively, where $\langle\beta_t\rangle$ has not yet been introduced [29]. In panels (b) and (c), the ratios of data to fit are presented corresponding to the dotted and dashed curves respectively. Detailed information on Fig-

ure 3 and the related parameters can be found in ref. [29]. More figures can be found in refs. [29–31, 70], which studies various particles and jets produced in different collisions over an energy range from a few GeV to above 10 TeV.

In the above discussions, the particles, collisions, and energies are not distinguished deliberately. In fact, not only for baryons but also for leptons, one may use the same idea and formalism to fit their p_T spectra in wide range in different collisions at different energies [29–31, 70]. In particular, in most cases, the number of participant partons is defined by two. This is due to one projectile parton and one target parton being main participants. Even for the p_T spectra of various jets, one may use the convolution of two revised Tsallis-like functions to fit them [70]. The third participant parton maybe is needed to revise the result of two participant partons. From small system such as hadron-hadron and hadron-nucleus collisions to large system such as nucleus-nucleus collisions, the idea and formalism are the same. This sameness is a reflection of the similarity, commonality, and universality existed in high energy collisions [4–11]. This enlightens that the contributions of contributor partons for different particles in different collisions are considered.

In addition, not only for the spectra in low- p_T region which is contributed by the soft excitation process, but also for the spectra in high- p_T region which is contributed by the hard scattering process, one has uniformly used the same idea and formalism. In the framework of multi-source thermal model at the parton level, both the processes are considered due to the contributions of contributor partons. There is no obvious difference for the two processes, but the violent degree. This sameness is also a reflection of the similarity, commonality, and universality existed in high energy collisions [4–11].

Before summary and conclusion, it should be emphasized that the parameter $\langle\beta_t\rangle$ is the average transverse flow velocity at the parton level. Although both p_T and y can be deformed by the presence of collective flow, a suitable description for the spectrum of particles naturally includes the influence of collective flow. As a constant value for given spectrum, $\langle\beta_t\rangle$ is independent of p_T . However, $\langle\beta_t\rangle$ depends on y due to the fact that the spectrum depends on y . The introduction of $\langle\beta_t\rangle$ in Eqs. (36)–(38) is based on the Lorentz-like transformation, in which $\langle\beta_t\rangle$ is also the average transverse velocity of the motion reference system which reflects the collective flow. This treatment is different from the blast-wave model [82–85], though the results are not contradictory.

Although there are many works already done on analysis and on the interpretation of the Tsallis statistics

role in high energy collisions [65–69], the improvement of the present work is significant. 1) The revised index a_0 which flexibly describes the winding degree of the spectra in low- p_T region is introduced, in which the contribution of resonance generation is significant. 2) The revised Tsallis-like function is used to describe the transverse momenta of the participant partons which contribute to p_T of particles, where various possible azimuths in the transverse plane are discussed. 3) The average transverse flow velocity is introduced, and the kinetic freeze-out temperature and average transverse flow velocity are conveniently obtained at the parton level.

IV. SUMMARY AND CONCLUSION

To see the method for describing the transverse momentum spectra of final-state particles produced in high energy collisions, the physics picture and formalism expression treated in the framework of multi-source thermal model at the parton level has been reviewed. Generally, two or three partons contribute to the transverse momentum spectra of mesons or baryons, while two partons contribute to the transverse momentum spectra of leptons or jets.

In general case, the difference between the parton azimuths is variant in $[0, 2\pi]$. The Monte Carlo method may be used to perform the calculations. If the difference is 0 or π , one may obtain a convolution of two or three probability density functions, which is an analytical expression. If the difference is $\pi/2$, one may also obtain an analytical expression if one integrates azimuthal variable over the united probability density function of transverse momentum and azimuth.

The fitting experience shows that the convolution of two or three probability density functions is more

suitable in describing the particle transverse momentum spectra, though the various differences between the parton azimuths sounds more reasonable. The transverse momentum spectra in different collisions are uniformly described at the parton level. The same contributor partons reflect the origin of the similarity, commonality, and universality existed in high energy collisions.

Data Availability

The data used to support the findings of this study are included within the article and are cited at relevant places within the text as references.

Ethical Approval

The authors declare that they are in compliance with ethical standards regarding the content of this paper.

Disclosure

The funding agencies have no role in the design of the study; in the collection, analysis, or interpretation of the data; in the writing of the manuscript; or in the decision to publish the results.

Conflicts of Interest

The authors declare that there are no conflicts of interest regarding the publication of this paper.

Acknowledgments

This work was supported by the National Natural Science Foundation of China under Grant Nos. 12147215, 12047571, 11575103, and 11947418, the Scientific and Technological Innovation Programs of Higher Education Institutions in Shanxi (STIP) under Grant No. 201802017, the Shanxi Provincial Natural Science Foundation under Grant No. 201901D111043, and the Fund for Shanxi “1331 Project” Key Subjects Construction.

[1] H. Wang, J.-H. Chen, Y.-G. Ma, and S. Zhang, “Charm hadron azimuthal angular correlations in Au+Au collisions at $\sqrt{s_{NN}} = 200$ GeV from parton scatterings,” *Nuclear Science and Techniques*, vol. 30, no. 12, article 185, 2019.

[2] Z.-B. Tang, W.-M. Zha, and Y.-F. Zhang, “An experimental review of open heavy flavor and quarkonium production at RHIC,” *Nuclear Science and Techniques*, vol. 31, no. 8, article 81, 2020.

[3] Y.-C. Liu and X.-G. Huang, “Anomalous chiral transports and spin polarization in heavy-ion collisions,” *Nuclear Science and Techniques*, vol. 31, no. 6, article 56,

2020.

[4] E. K. G. Sarkisyan and A. S. Sakharov, “Multihadron production features in different reactions,” Invited talk at the XXXV International Symposium on Multiparticle Dynamics (ISMD 05), Kromeriz, Czech Republic, 9–15 Aug. 2005, *AIP Conference Proceedings*, vol. 828, pp. 35–41, 2006.

[5] E. K. G. Sarkisyan and A. S. Sakharov, “Relating multihadron production in hadronic and nuclear collisions,” *The European Physical Journal C*, vol. 70, no. 3, pp. 533–541, 2010.

[6] A. N. Mishra, R. Sahoo, E. K. G. Sarkisyan, and A.

- S. Sakharov, “Effective-energy budget in multiparticle production in nuclear collisions,” *The European Physical Journal C*, vol. 74, no. 11, article 3147, 2014 and “Erratum,” *ibid.*, vol. 75, no. 2, article 70, 2015.
- [7] E. K. G. Sarkisyan, A. N. Mishra, R. Sahoo, and A. S. Sakharov, “Multihadron production dynamics exploring the energy balance in hadronic and nuclear collisions,” *Physical Review D*, vol. 93, no. 5, article 054046, 2016 and “Erratum,” *ibid.*, vol. 93, no. 7, article 079904, 2016.
- [8] E. K. G. Sarkisyan, A. N. Mishra, R. Sahoo, and A. S. Sakharov, “Centrality dependence of midrapidity density from GeV to TeV heavy-ion collisions in the effective-energy universality picture of hadroproduction,” *Physical Review D*, vol. 94, no. 1, article 011501(R), 2016.
- [9] E. K. G. Sarkisyan, A. N. Mishra, R. Sahoo, and A. S. Sakharov, “Effective-energy universality approach describing total multiplicity centrality dependence in heavy-ion collisions,” *EPL (Europhysics Letters)*, vol. 127, no. 6, article 62001, 2019.
- [10] A. N. Mishra, A. Ortiz, and G. Paic, “Intriguing similarities of high- p_T particle production between pp and A - A collisions,” *Physical Review C*, vol. 99, no. 3, article 034911, 2019.
- [11] P. Castorina, A. Iorio, D. Lanteri, H. Satz, and M. Spousta, “Universality in hadronic and nuclear collisions at high energy,” *Physical Review C*, vol. 101, no. 5, article 054902, 2020.
- [12] F.-H. Liu, “Unified description of multiplicity distributions of final-state particles produced in collisions at high energies,” *Nuclear Physics A*, vol. 810, nos. 1–4, pp. 159–172, 2008.
- [13] F.-H. Liu and J.-S. Li, “Isotopic production cross section of fragments in $^{56}\text{Fe}+p$ and $^{136}\text{Xe}(^{124}\text{Xe})+Pb$ reactions over an energy range from 300A to 1500A MeV,” *Physical Review C*, vol. 78, no. 4, article 044602, 2008.
- [14] F.-H. Liu, “Dependence of charged particle pseudorapidity distributions on centrality and energy in $p(d)A$ collisions at high energies,” *Physical Review C*, vol. 78, no. 1, article 014902, 2008.
- [15] F.-H. Liu, B. K. Singh, and N. N. Abd Allah, “Integral frequency distribution of projectile alpha fragments in nuclear multifragmentations at intermediate and high energies,” *Nuclear Physics B (Proceedings Supplements)*, vols. 175–176, pp. 54–57, 2008.
- [16] F.-H. Liu, Q.-W. Lü, B.-C. Li, and R. Bekmirzaev, “A description of the multiplicity distributions of nuclear fragments in hA and AA collisions at intermediate and high energies,” *Chinese Journal of Physics*, vol. 49, no. 2, pp. 601–620, 2011.
- [17] W. Y. Chang, “Jets induced in emulsion and cloud chambers by cosmic ray particles of energy (10^{11} – 10^{14} eV),” *Acta Physica Sinica*, vol. 17, no. 8, pp. 9–33, 1961.
- [18] G. D. Westfall, J. Gosset, P. J. Johansen, A. M. Poskanzer, W. G. Meyer, H. H. Gutbrod, A. Sandoval, and R. Stock, “Nuclear fireball model for proton inclusive spectra from relativistic heavy-ion collisions,” *Physical Review Letters*, vol. 37, no. 18, pp. 1202–1205, 1976.
- [19] G. Ingrosso and P. Rotelli, “Three-fireball model of π^-p inelastic interactions at 205 GeV/c,” *Il Nuovo Cimento A*, vol. 41, no. 2, pp. 233–249, 1977.
- [20] A. D’Innocenzo, G. Ingrosso, and P. Rotelli, “The $p\bar{p}$ annihilation channel as a prototype for the central fireball in pp production processes,” *Lettere al Nuovo Cimento*, vol. 25, no. 13, pp. 393–398, 1979.
- [21] A. D’Innocenzo, G. Ingrosso, and P. Rotelli, “The three-component fireball model and pp interactions,” *Lettere al Nuovo Cimento*, vol. 27, no. 14, pp. 457–466, 1980.
- [22] A. D’Innocenzo, G. Ingrosso, and P. Rotelli, “A universal scaling function for hadron-hadron interactions,” *Il Nuovo Cimento A*, vol. 55, no. 4, pp. 417–436, 1980.
- [23] K.-C. Chou, L.-S. Liu, and T.-C. Meng, “Koba-Nielsen-Olesen scaling and production mechanism in high-energy collisions,” *Physical Review D*, vol. 28, no. 5, pp. 1080–1085, 1983.
- [24] L.-S. Liu and T.-C. Meng, “Multiplicity and energy distributions in high-energy e^+e^- , pp , and $p\bar{p}$ collisions,” *Physical Review D*, vol. 27, no. 11, pp. 2640–2647, 1983.
- [25] F.-H. Liu, J.-S. Li, and M.-Y. Duan, “Light fragment emission in ^{86}Kr - ^{124}Sn collisions at 25 MeV/nucleon,” *Physical Review C*, vol. 75, no. 5, article 054613, 2007.
- [26] F.-H. Liu, “Particle pseudorapidity distribution in Au-Au collisions at $\sqrt{s} = 130A$ GeV,” *Physical Review C*, vol. 66, no. 4, article 047902, 2002.
- [27] F.-H. Liu, “Particle production in Au-Au collisions at RHIC energies,” *Physics Letters B*, vol. 583, nos. 1–2, pp. 68–72, 2004.
- [28] F.-H. Liu, Y.-Q. Gao, T. Tian, and B.-C. Li, “Unified description of transverse momentum spectrums contributed by soft and hard processes in high-energy nuclear collisions,” *The European Physical Journal A*, vol. 50, no. 6, article 94, 2014.
- [29] P.-P. Yang, F.-H. Liu, and R. Sahoo, “A new description of transverse momentum spectra of identified particles produced in proton-proton collisions at high energies,” *Advances in High Energy Physics*, vol. 2020, article 6742578, 2020.
- [30] P.-P. Yang, M.-Y. Duan, and F.-H. Liu, “Dependence of related parameters on centrality and mass in a new treatment for transverse momentum spectra in high energy collisions,” *The European Physical Journal A*, vol. 57, no. 2, article 63, 2021.
- [31] L.-L. Li, F.-H. Liu, and Kh. K. Olimov, “Excitation functions of Tsallis-like parameters in high-energy nucleus-nucleus collisions,” *Entropy*, vol. 23, no. 4, article 478, 2021.
- [32] F.-H. Liu, Y.-Q. Gao, H.-R. Wei, “On descriptions of particle transverse momentum spectra in high energy collisions,” *Advances in High Energy Physics*, vol. 2014, article 293873, 2014.
- [33] L.-L. Li and F.-H. Liu, “Kinetic freeze-out properties from transverse momentum spectra of pions in high energy proton-proton collisions,” *Physics*, vol. 2, no. 2, pp. 277–308, 2020.
- [34] T. Chujo, “Excitation functions of baryon anomaly and

- freeze-out properties at RHIC-PHENIX,” *Journal of Physics G*, vol. 34, no. 8, pp. S893–S896, 2007.
- [35] H. Petersen, J. Steinheimer, M. Bleicher, and H. Stoecker, “ $\langle m_T \rangle$ excitation function: Freeze-out and equation of state dependence,” *Journal of Physics G*, vol. 36, no. 5, article 055104, 2009.
- [36] J. Cleymans, H. Oeschler, K. Redlich, and S. Wheaton, “Strangeness excitation functions and transition from baryonic to mesonic freeze-out,” *Acta Physica Polonica B Proceedings Series*, vol. 3, no. 3, pp. 533–538, 2010.
- [37] Y. Nara and H. Stoecker, “Sensitivity of the excitation functions of collective flow to relativistic scalar and vector meson interactions in the relativistic quantum molecular dynamics model RQMD.RMF,” *Physical Review C*, vol. 100, no. 5, article 054902, 2019.
- [38] V. Kolesnikov, V. Kireyeu, V. Lenivenko, A. Mudrokh, K. Shtejer, D. Zinchenko, and E. Bratkovskaya, “A new review of excitation functions of hadron production in pp collisions in the NICA energy range,” *Physics of Particles and Nuclei Letters*, volume 17, no. 2, pp. 142–153, 2020.
- [39] I. Arsene, I. G. Bearden, D. Beavisa et al. (BRAHMS Collaboration), “Quark-gluon plasma and color glass condensate at RHIC? The perspective from the BRAHMS experiment,” *Nuclear Physics A*, vol. 757, nos. 1–2, pp. 1–27, 2005.
- [40] B. B. Back, M. D. Baker, M. Ballintijn et al. (PHOBOS Collaboration), “The PHOBOS perspective on discoveries at RHIC,” *Nuclear Physics A*, vol. 757, nos. 1–2, pp. 28–101, 2005.
- [41] J. Adams, M. M. Aggarwal, Z. Ahammed et al. (STAR Collaboration), “Experimental and theoretical challenges in the search for the quark-gluon plasma: The STAR Collaboration’s critical assessment of the evidence from RHIC collisions,” *Nuclear Physics A*, vol. 757, nos. 1–2, pp. 102–183, 2005.
- [42] K. Adcox, S. S. Adler, and S. Afanasiev et al. (PHENIX Collaboration), “Formation of dense partonic matter in relativistic nucleus-nucleus collisions at RHIC: Experimental evaluation by the PHENIX Collaboration,” *Nuclear Physics A*, vol. 757, nos. 1–2, pp. 184–283, 2005.
- [43] K. Zapp, G. Ingelman, J. Rathsman, and J. Stachel, “Heavy quark energy loss through soft QCD scattering in the QGP,” *International Journal of Modern Physics E*, vol. 16, no. 8, pp. 2072–2078, 2007.
- [44] I. Kuznetsova and J. Rafelski, “Non-equilibrium heavy flavored hadron yields from chemical equilibrium strangeness-rich QGP,” *Journal of Physics G*, vol. 35, no. 4, article 044043, 2008.
- [45] Z.-W. Lin, H. L. Li, and F. Q. Wang, “Heavy quark flow as better probes of QGP properties,” *EPJ Web of Conferences*, vol. 171, article 19005, 2018.
- [46] B. V. Jacak, “Quark matter: Status and challenges,” *Nuclear Physics A*, vol. 1005, article 122052, 2021.
- [47] C. Shen, “Studying QGP with flow: A theory overview,” *Nuclear Physics A*, vol. 1005, article 121788, 2021.
- [48] K. K. Gajdosová, “Probing QGP with flow: An experimental overview,” *Nuclear Physics A*, vol. 1005, article 121802, 2021.
- [49] K. J. Eskola, “Pre-thermalization dynamics: initial conditions for QGP at the LHC and RHIC from perturbative QCD,” *Progress of Theoretical Physics Supplement*, vol. 129, pp. 1–10, 1997.
- [50] K. J. Eskola, “Initial state of the QGP from perturbative QCD + saturation,” *Nuclear Physics A*, vol. 702, nos. 1–4, pp. 249–258, 2002.
- [51] J. Letessier and J. Rafelski, “QCD equations of state and the QGP liquid model,” *Physical Review C*, vol. 67, no. 3, article 031902, 2003.
- [52] H. Satz, “Critical behaviour in statistical QCD,” *International Journal of Modern Physics A*, vol. 21, no. 4, pp. 672–681, 2006.
- [53] L. S. Kisslinger, “Review of QCD, QGP, heavy quark meson production enhancement and suppression,” *International Journal of Modern Physics A*, vol. 32, no. 15, article 1730008, 2017.
- [54] G. Q. Li, C. M. Ko, and G. E. Brown, “Effects of in-medium vector meson masses on low-mass dileptons from SPS heavy-ion collisions,” *Nuclear Physics A*, vol. 606, nos. 3–4, pp. 568–606, 1996.
- [55] G. Q. Li, C. M. Ko, G. E. Brown, and H. Sorge, “Dilepton production in proton-nucleus and nucleus-nucleus collisions at SPS energies,” *Nuclear Physics A*, vol. 611, no. 4, pp. 539–567, 1996.
- [56] A. Bieniek, “Modification of the π - ω - ρ vertex in nuclear medium and its influence on the dilepton production rate in relativistic heavy-ion collisions,” arXiv:nucl-th/0411084, 2004.
- [57] B.-W. Zhang, C. M. Ko, and W. Liu, “Thermal charm production in quark-gluon plasma at LHC,” *Physical Review C*, vol. 77, no. 2, article 024901, 2008.
- [58] Z.-J. Xiao and C.-D. Lü, *Introduction to Particle Physics*, Science Press, Beijing, China, 2016.
- [59] P. Desgrolard, M. Giffon, and E. Martynov, “Elastic pp and $\bar{p}p$ scattering in the Modified Additive Quark Model,” *The European Physical Journal C*, vol. 18, no. 12, pp. 359–367, 2000.
- [60] Yu. M. Shabelski and A. G. Shuvaev, “Midrapidity inclusive densities in high energy pp collisions in additive quark model,” *The European Physical Journal C*, vol. 76, no. 8, article 470, 2016.
- [61] Yu. M. Shabelski and A. G. Shuvaev, “Real part of pp scattering amplitude in Additive Quark Model at LHC energies,” *The European Physical Journal C*, vol. 78, no. 6, article 497, 2018.
- [62] G. H. Arakelyan, Yu. M. Shabelski, and A. G. Shuvaev, “Central and peripheral hadron-nucleus collisions in the Additive Quark Model,” arXiv:1805.11293 [hep-ph], 2018.
- [63] P.-P. Yang, Q. Wang, and F.-H. Liu, “Mutual derivation between arbitrary distribution forms of momenta and momentum components,” *International Journal of Theoretical Physics*, vol. 58, no. 8, pp. 2603–2618, 2019.
- [64] G.-R. Zhou, *Probability Theory and Mathematical Statistics*, Higher Education Press, Beijing, China, 1984.

- [65] C. Tsallis, “Possible generalization of Boltzmann-Gibbs statistics,” *Journal of Statistical Physics*, vol. 52, nos. 1–2, pp. 479–487, 1988.
- [66] T. S. Biró, G. Purcsel, K. Ürmösy, “Non-extensive approach to quark matter,” *The European Physical Journal A*, vol. 40, no. 3, pp. 325–340, 2009.
- [67] J. Cleymans and D. Worku, “Relativistic thermodynamics: Transverse momentum distributions in high-energy physics,” *The European Physical Journal A*, vol. 48, no. 11, article 160, 2012.
- [68] H. Zheng and L. L. Zhu, “Comparing the Tsallis distribution with and without thermodynamical description in $p+p$ collisions,” *Advances in High Energy Physics*, vol. 2016, article 9632126, 2016.
- [69] J. Cleymans and M. W. Paradza, “Tsallis statistics in high energy physics: Chemical and thermal freeze-outs,” *Physics*, vol. 2, no. 4, pp. 654–664, 2020.
- [70] Y.-M. Tai, P.-P. Yang, F.-H. Liu, “An analysis of transverse momentum spectra of various jets produced in high energy collisions,” *Advances in High Energy Physics*, vol. 2021, article 8832892, 2021.
- [71] S. Takeuchi, K. Murase, T. Hirano et al., “Effects of hadronic rescattering on multistrange hadrons in high-energy nuclear collisions,” *Physical Review C*, vol. 92, no. 4, article 044907, 2015.
- [72] H. Heiselberg and A. M. Levy, “Elliptic flow and Hanbury-Brown-Twiss in noncentral nuclear collisions,” *Physical Review C*, vol. 59, no. 5, pp. 2716–2727, 1999.
- [73] U. W. Heinz, “Concepts of heavy-ion physics,” Lecture Notes for Lectures Presented at the 2nd CERN-Latin-American School of High-Energy Physics, June 1–14, 2003 (San Miguel Regla, Mexico, 2004), arXiv:hep-ph/0407360, 2004.
- [74] R. Russo, “Measurement of D^+ meson production in p -Pb collisions with the ALICE detector,” Ph.D. thesis (Universita degli Studi di Torino, Italy, 2015), arXiv:1511.04380 [nucl-ex], 2015.
- [75] H.-R. Wei, F.-H. Liu, and R. A. Lacey, “Kinetic freeze-out temperature and flow velocity extracted from transverse momentum spectra of final-state light flavor particles produced in collisions at RHIC and LHC,” *The European Physical Journal A*, vol. 52, no. 4, article 102, 2016.
- [76] H.-R. Wei, F.-H. Liu, and R. A. Lacey, “Disentangling random thermal motion of particles and collective expansion of source from transverse momentum spectra in high energy collisions,” *Journal of Physics G*, vol. 43, no. 12, article 125102, 2016.
- [77] Kh. K. Olimov, A. Iqbal, and S. Masood, “Systematic analysis of midrapidity transverse momentum spectra of identified charged particles in $p+p$ collisions at $(s_{nn})^{1/2} = 2.76, 5.02, \text{ and } 7 \text{ TeV}$ at the LHC,” *International Journal of Modern Physics A*, vol. 35, no. 27, article 2050167, 2020.
- [78] Kh. K. Olimov, S. Z. Kanokova, K. Olimov, K. G. Gulamov, B. S. Yuldashev, S. L. Lutpullaev, and F. Y. Umarov, “Average transverse expansion velocities and global freeze-out temperatures in central Cu+Cu, Au+Au, and Pb+Pb collisions at high energies at RHIC and LHC,” *Modern Physics Letters A*, vol. 35, no. 14, article 2050115, 2020.
- [79] Kh. K. Olimov, S. Z. Kanokova, A. K. Olimov, K. I. Umarov, B. J. Tukhtaev, K. G. Gulamov, B. S. Yuldashev, S. L. Lutpullaev, N. Sh. Saidkhanov, K. Olimov, and T. Kh. Sadykov, “Combined analysis of midrapidity transverse momentum spectra of the charged pions and kaons, protons and antiprotons in $p+p$ and Pb+Pb collisions at $(s_{nn})^{1/2} = 2.76 \text{ and } 5.02 \text{ TeV}$ at the LHC,” *Modern Physics Letters A*, vol. 35, no. 29, article 2050237, 2020.
- [80] Kh. K. Olimov, K. I. Umarov, A. Iqbal, S. Masood, and F.-H. Liu, “Analysis of midrapidity transverse momentum distributions of the charged pions and kaons, protons and antiprotons in $p+p$ collisions at $(s_{nn})^{1/2} = 2.76, 5.02, \text{ and } 7 \text{ TeV}$ at the LHC,” *Proceedings of the International Conference on “Fundamental and Applied Problems of Physics”*, pp. 78–83, Tashkent, Uzbekistan, September 22–23, 2020.
- [81] A. Adare et al. (PHENIX Collaboration), “Measurement of neutral mesons in $p+p$ collisions at $\sqrt{s} = 200 \text{ GeV}$ and scaling production,” *Physical Review D*, vol. 83, no. 5, article 052004, 2011.
- [82] E. Schnedermann, J. Sollfrank, and U. Heinz, “Thermal phenomenology of hadrons from 200A GeV S+S collisions,” *Physical Review C*, vol. 48, no. 5, pp. 2462–2475, 1993.
- [83] B. I. Abelev et al. (STAR Collaboration), “Systematic measurements of identified particle spectra in $pp, d+Au,$ and $Au+Au$ collisions at the STAR detector,” *Physical Review C*, vol. 79, no. 3, article 034909, 2009.
- [84] Z. B. Tang, Y. C. Xu, L. J. Ruan, G. van Buren, F. Q. Wang, and Z. B. Xu, “Spectra and radial flow in relativistic heavy ion collisions with Tsallis statistics in a blastwave description,” *Physical Review C*, vol. 79, no. 5, article 051901(R), 2009.
- [85] B. I. Abelev et al. (STAR Collaboration), “Identified particle production, azimuthal anisotropy, and interferometry measurements in $Au+Au$ collisions at $\sqrt{s_{NN}} = 9.2 \text{ GeV}$,” *Physical Review C*, vol. 81, no. 2, article 024911, 2010.